**Neuron, Volume *104***

## Supplemental Information

# A Neural Circuit Arbitrates between Persistence and Withdrawal in Hungry *Drosophila*

**Sercan Sayin, Jean-Francois De Backer, K.P. Siju, Marina E. Wosniack, Laurence P. Lewis, Lisa-Marie Frisch, Benedikt Gansen, Philipp Schlegel, Amelia Edmondson-Stait, Nadiya Sharifi, Corey B. Fisher, Steven A. Calle-Schuler, J. Scott Lauritzen, Davi D. Bock, Marta Costa, Gregory S.X.E. Jefferis, Julijana Gjorgjieva, and Ilona C. Grunwald Kadow**

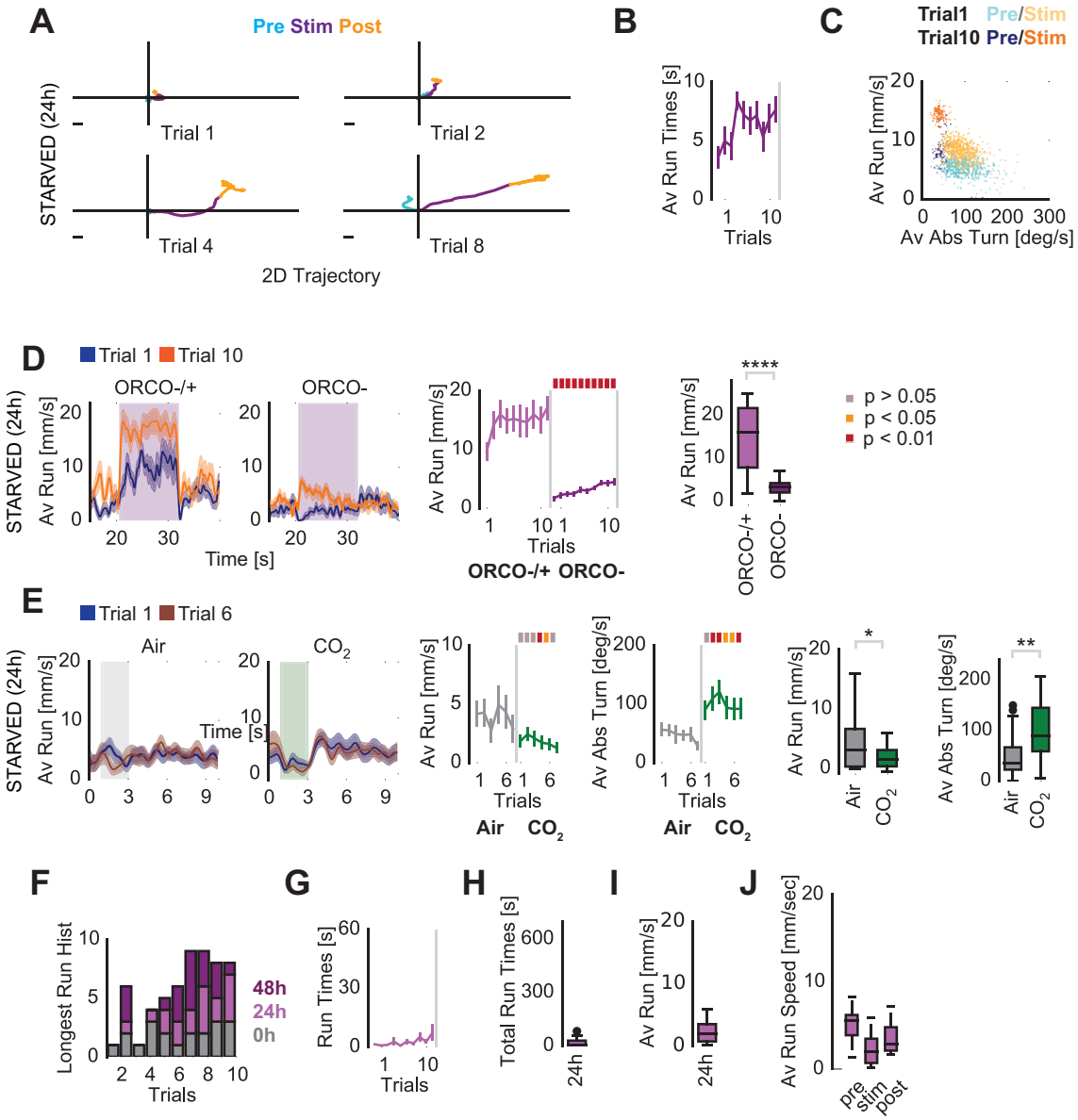


**Fig. S1. Related to Fig. 1**

(A) Reconstructed 2D trajectory of a representative fly during single trials. The pre- and post-stimulation behavior for 12 s were depicted in cyan and yellow, respectively, and odor-tracking behavior for 12 s in purple. All trials aligned at the origin for the odor onset. Over trials, the fly showed an increased persistence in running. The locomotion trajectory data were plotted against pseudo-cardinal coordinates and smoothened with Butterworth filter for visualization. (B) Average running time lengths during the first bout of running upon start of vinegar exposure. Longer running bouts were observed over trials. (C) Evolution of the two-dimensional behavioral space on the spherical treadmill, constructed from 100 ms chunks of average running and absolute turning of 18 flies. Given the choice of run or turn, in average, flies executed turns in higher probability during in pre-stimulation period in the first trial (dark and light blue) than in the last trial (dark and light orange). The

odor exposure shifted behavioral to longer runs at later trials from more turns at earlier trials. (D) left: Running behavior of food-deprived Orco null (Orco -) and heterozygous (Orco -/+) mutants. Right: Average running speed of Orco null and heterozygous mutants for vinegar over ten trials (N=10/10, 2-way RM ANOVA p(trials)<0.0001, p(groups)<0.0001, p(interaction)=0.0562). The boxplot displays the main group effect of the ANOVA. (E) Behavior during aversive odor presentation. Panel 1 and 2 from left: Flies were exposed to alternating $CO_2$ and air plumes to prevent an anesthetizing effect of $CO_2$ over six trials. Panel 3: Repeated stimulation with $CO_2$ gradually decreased average running speed over trials. Panel 4: Flies slowed down at contact with aversive $CO_2$. Average running speed under $CO_2$ exposure was significantly lower than the speed observed during air exposure. Panel 5: Flies executed escape turns under $CO_2$ as they turned significantly more (N=10/10, *Running speed*: 2-way RM ANOVA, matching for both factors, p(trials)=0.4046; p(groups)=0.0262, p(interaction)=0.45; *Turn*: 2-way RM ANOVA, matching for both factors, p(trials)=0.38; p(groups)=0.0045, p(interaction)=0.51). Boxplots represent the main group effects of the respective ANOVAs. (F) Histogram for trials in which flies performed respective longest running bouts throughout 10 trials. The longest run bouts were distributed over trials. For 24 hours starvation, the most frequent peak was observed in the $8^{th}$ and $10^{th}$ trials, whereas 48h starvation experimental group reached its peak at the $7^{th}$ trial. Satiated flies exhibited a random distribution (N=20/18/19). (G) Closed loop experiment with 24 h starved flies stimulated with air instead of vinegar odor during stimulus phase. Flies run only short times at every trial with very little change over trials. (H) Box plot showing the total average run time over 10 trials. (I) Box plot showing average speed over all trials during stimulus phase. (J) Box plots comparing average speed over all trials during pre, post and stimulus phase. Note that there is no significant difference in speed between the different phases. N=9 flies, 24h starved.

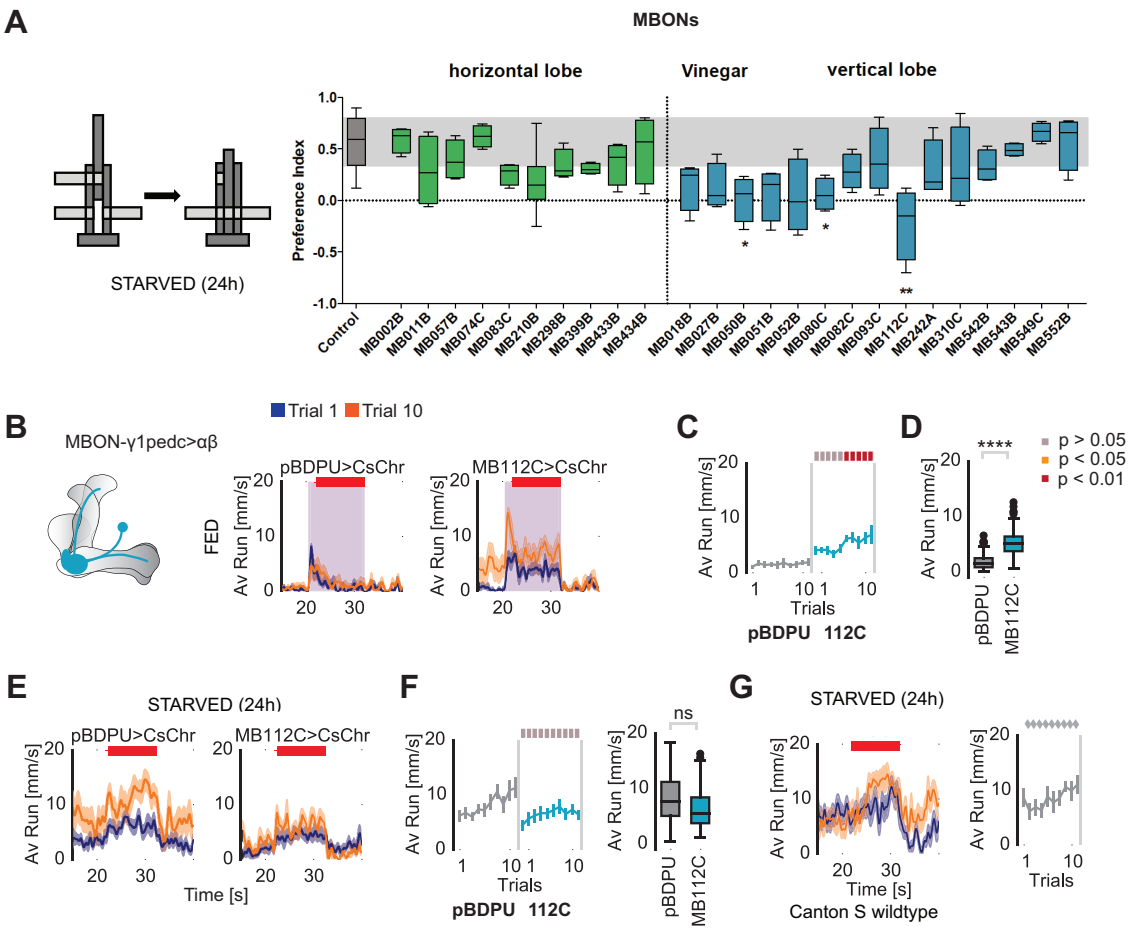


**Fig. S2. Related to Fig. 2**

(A) T-maze neuronal silencing screen for mushroom body output neurons (MBONs) and Kenyon cells subtypes required for innate vinegar attraction. MB Split-Gal4 lines were screened with the UAS-Shibire$^{ts1}$ effector at the non-permissive temperature of 30$^{o}$C (N=4-12 for experimental groups, controls were pooled to an N of 48, Kruskal-Wallis test and Dunn's post-hoc test). (B) Running speeds in fed flies when MB112C was activated via optogenetics (*MB112C>UAS-CsChrimson*). Activation of MBON-γ1pdec>αβ increased odor tracking behavior significantly (Control: *pBDPU-Gal4>UAS-CsChrimson*). (C) Running speeds during stimulus phase over trials (N=10/10, 2-way RM ANOVA, p(trials)=0.0335, p(groups)<0.0001, p(interaction)=0.21). (D) Average running speed over all trials during the stimulus phase. (E) Running speed averages for the light only condition of *MB112C>UAS-CsChrimson* and empty-Gal4 control (*pBDPU-Gal4>UAS-CsChrimson*) animals. (F) MBON-γ1pedc>αβ activation in starved flies did not induce locomotion or tracking compared to the control flies in the absence of odor stimulation (N=10/10, 2-way RM ANOVA p(trials)<0.0001, p(groups)=0.20, p(interaction)=0.10). (G) Wild-type control flies show a mild, but not significant, increase in motility and locomotion under 617nm, 30μW/mm2 light delivery (N=10, one-way RM ANOVA p=0.10). The flies are presumably attracted to the light in the absence of CsChrimson expression. For all analyses, running speeds over trials are represented as mean ± SEM with Sidak's trial-to-trial comparisons

displayed as color-coded p-values. Boxplots represent the main group effect of the 2-way ANOVA. Statistical notations are as follows: ‘ns’ $p > 0.05$, ‘***’ $p < 0.001$, ‘****’ $p < 0.0001$.

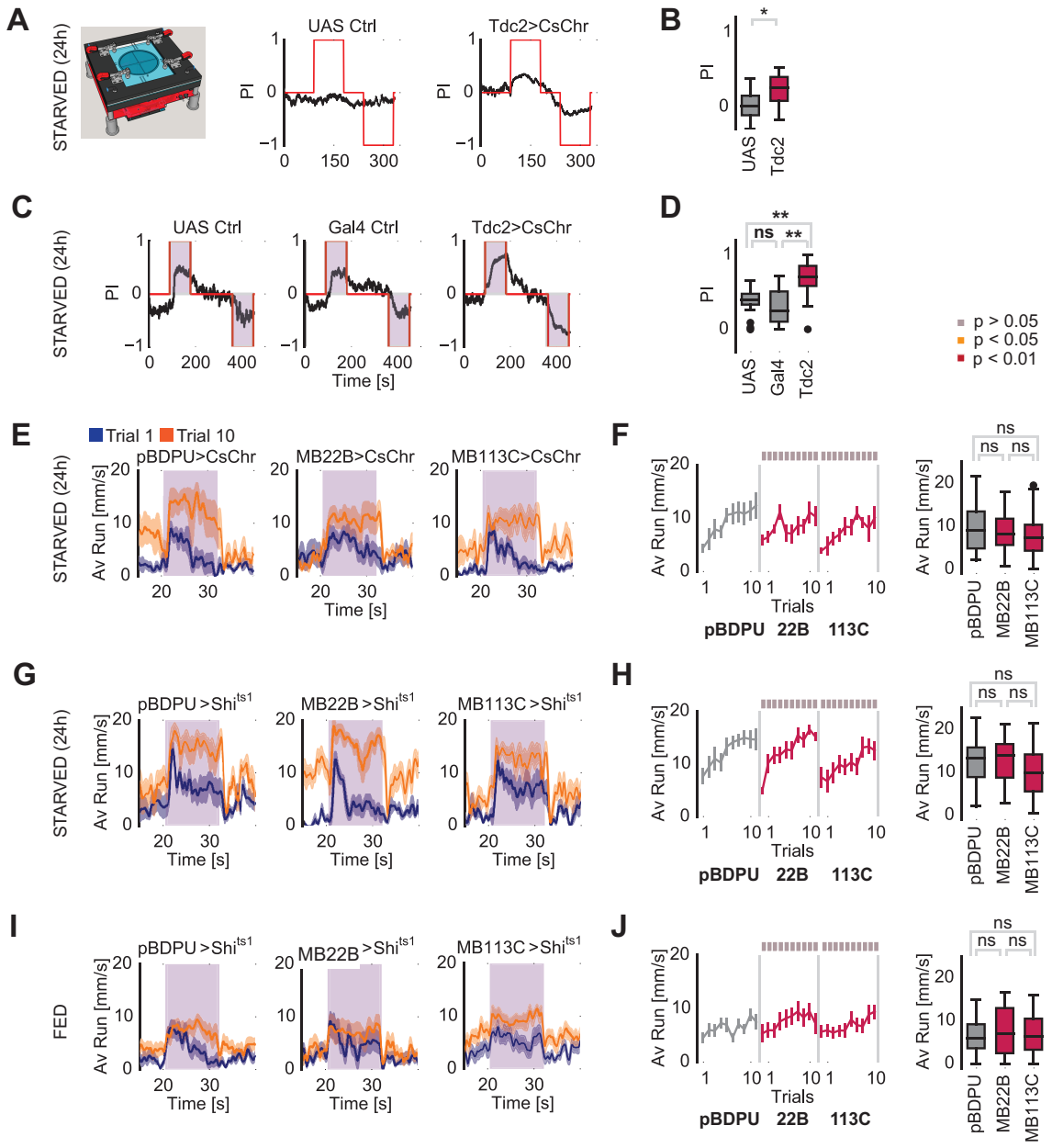


**Fig. S3. Related to Fig. 5**

(A) left: Scheme of optogenetic and olfactory behavioral test arena. Right: Average preference index during optogenetic activation of octopaminergic neurons. (B) Activation of all OANs (*Tdc2>UAS-CsChrimson*) led to a significantly higher accumulation of flies in the illuminated quadrants when compared to genetic controls (N=16/16, one-way ANOVA, $p<0.05$, with Tukey's HSD post hoc analysis). (C) Average preference index during optogenetic activation of octopaminergic neurons under vinegar exposure. (D) Activation of all OANs (*Tdc2>UAS-CsChrimson*) led to a significantly higher accumulation of flies in the odor+light quadrants when compared to genetic controls (N=16/16/16, one-way ANOVA, $p=0.0001$, with Tukey's HSD post hoc analysis). (C) Running speeds for VPM

lines (*MB22B>UAS-CsChrimson* and *MB113C>UAS-CsChrimson*) and the control (*pBDPU-Gal4>UAS-CsChrimson*) with odor only exposure during trial 1 and 10. (D) Average running speeds over trials of *MB22B>UAS-CsChrimson* and *MB113C>UAS-CsChrimson* flies under vinegar in the absence of optogenetic stimulation compared to control (N=10/10/10, 2-way RM ANOVA p(trials)<0.0001, p(groups)=0.65, p(interaction)=0.20). (E) Running speeds for starved VPM lines (*MB22B>UAS-shi$^{ts1}$* and *MB113C>UAS-shi$^{ts1}$*) and the control (*pBDPU-Gal4>UAS-shi$^{ts1}$*) during trial 1 and 10. (F) Average running speeds over trials of starved *MB22B> UAS-shi$^{ts1}$* and *MB113C> UAS-shi$^{ts1}$* flies under vinegar compared to control (N=10/10/10, 2-way RM ANOVA p(trials)<0.0001, p(groups)=0.33, p(interaction)=0.14). (G) Running speeds for fed VPM lines (*MB22B>UAS-shi$^{ts1}$* and *MB113C> UAS-shi$^{ts1}$*) and the control (*pBDPU-Gal4> UAS-shi$^{ts1}$*) during trial 1 and 10. (H) Average running speeds over trials of fed *MB22B> UAS-shi$^{ts1}$* and *MB113C> UAS-shi$^{ts1}$* flies under vinegar compared to control (N=10/10/10, 2-way RM ANOVA p(trials)<0.0001, p(groups)=0.73, p(interaction)=0.40). For all analyses, running speeds over trials are represented as mean ± SEM with Tukey's trial-to-trial comparisons displayed as color-coded p-values. Boxplots represent the main group effect of the 2-way ANOVA. Statistical notations are as follows: 'ns' $p > 0.05$, '$**$' $p < 0.01$, '$***$' $p < 0.001$.

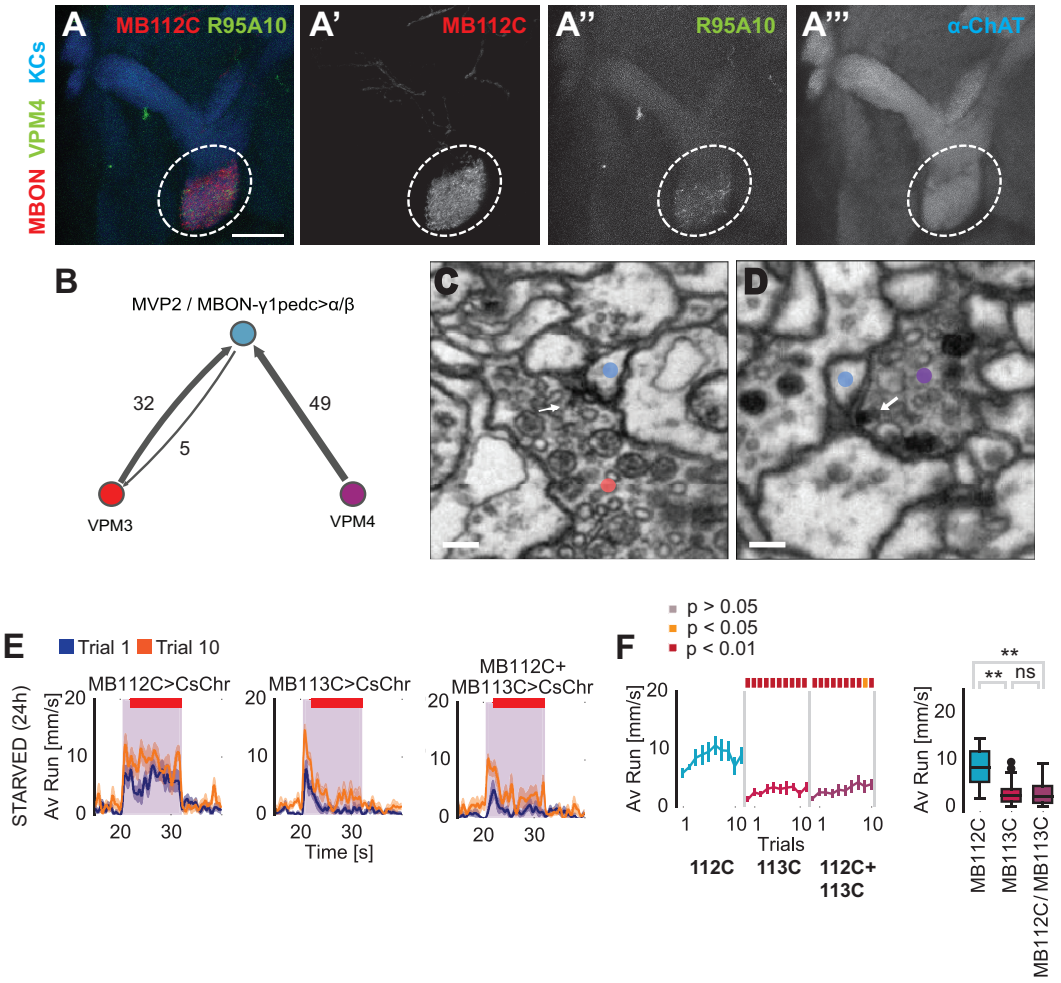


**Fig. S4. Related to Fig. 6**

(A-A''') Double stainings suggest that MBON-γ1pdec>αβ and VPM4 neurons could be synaptically connected. In the double labeling experiment, MBON-γ1pdec>αβ was visualized by *MB112C-Gal4>UAS-mCD8-RFP* (red) and VPM4 neurons were labeled by *GMR95A10-LexA>LexAop2-mCD8-GFP* (green). (A) Merged image displaying MBON-γ1pdec>αβ and VPM4 neurons. MB lobes are stained with anti-Chat (blue) (A'-''', single channels; 10µm scale bar. Note that VPM4 neurons innervate the dendritic region of MBON-γ1pdec>αβ at the level of the MB γ1 lobe region. (B) Wiring diagram of VPM3, VPM4 and MVP2 connectivity. Both VPM3 and VPM4 target MBON-γ1pdec>αβ dendrites in the γ1 compartment. Only VPM3 is reciprocally connected with MVP2. Numbers represent synapse counts. (C,D) Representative synapses (arrow) between VPM3 (red), VPM4 (purple) and MBON-γ1pdec>αβ (blue) show both clear core vesicles around the active zone as well as large dense core vesicles in close vicinity. 100 nm scale bar. (E) Running speeds for trial 1 and trial 10 of starved flies when MB112C and VPM4 neurons were activated via optogenetics simultaneously (*MB112C-Gal4; MB113C-Gal4 >UAS-CsChrimson*). (F) Activation of MBON-γ1pdec>αβ did not further increase appetitive odor response and tracking in starved animals. VPM4 and MBON-γ1pdec>αβ co-activation in

starved flies. Note that VPM4 activation completely suppresses odor tracking in the starved animal as seen also in the fed animal suggesting that VPM4 inhibits odor tracking regardless of starvation state (N=6/7/8; 2-way RM ANOVA p(trials)<0.0001, p(groups)=0.0004, p(interaction)=0.067). The boxplot displays the Tuckey's post hoc analysis on the main group effect. Running speeds over trials are represented as mean ± SEM with Tukey's trial-to-trial comparisons displayed as color-coded p-values. Statistical notations are as follows: 'ns' $p > 0.05$, '$**$' $p < 0.01$.

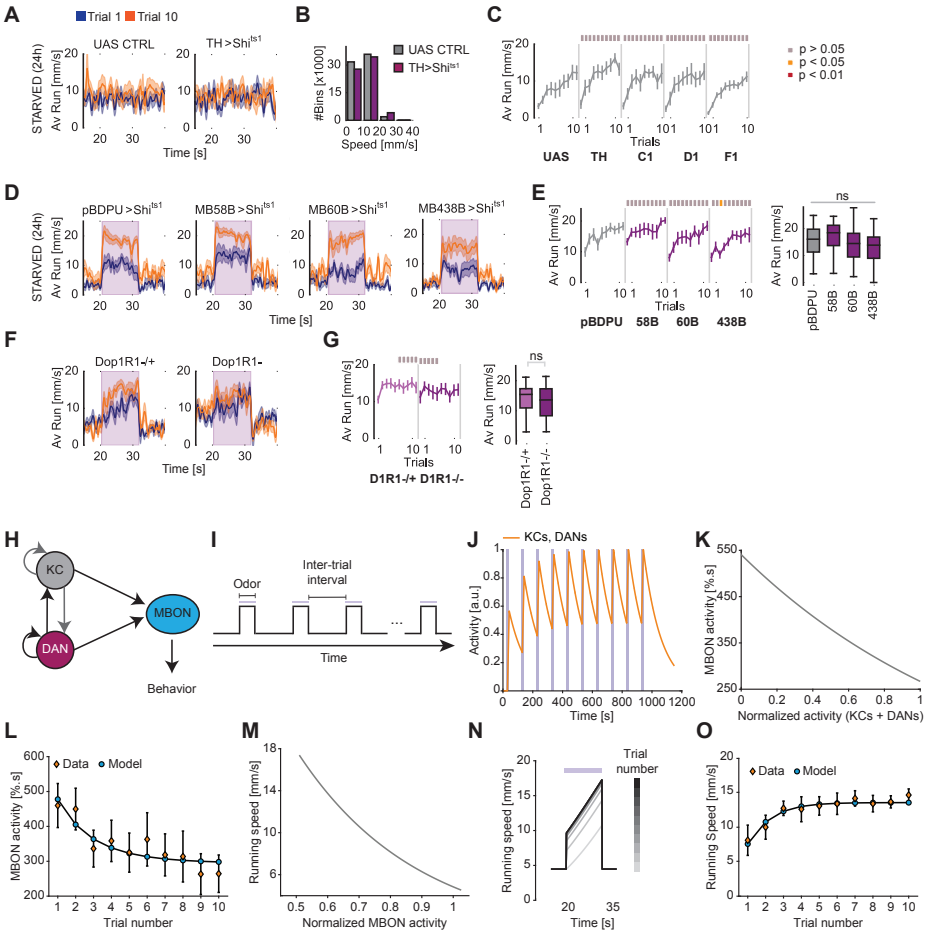


**Fig. S5. Related to Fig. 7**

(A) Flies carrying TH>shi$^{ts1}$ can move as fast as control flies over 10 trials at 35ºC and no odor stimulation. (B) Fly speeds were categorized into bins of different speeds. No difference was found between TH>shi$^{ts1}$ flies and controls (N=10/10; 2-way RM ANOVA p(trials)=0.0006, p(groups)=0.77, p(interaction)>0.99). (C) Running speed of hungry Gal4-control flies at trial 1 and 10 (24 h starved) of different TH-DAN subsets (*TH, C1, D1 and F1-Gal4>UAS-Shi$^{ts1}$*) compared to control (N=7/7/6/6/6; 2-way RM ANOVA p(trials)<0.0001, p(groups)=0.36, p(interaction)=0.43). See materials and methods for details on the lines. (D) Average running speed over 10 trials for hungry flies (24 h starved) with inactivated output of DANs (*MB-Gal4>UAS-Shi$^{ts1}$*) compared to control. (E) Running speed of hungry flies at trial 1 and 10 (24 h starved) with inactivated output of different DAN subsets (*MB-Gal4>UAS-Shi$^{ts1}$*) compared to control (N=8/8/9/8; 2-way RM ANOVA p(trials)<0.0001, p(groups)=0.32, p(interaction)=0.28). The boxplot display the Dunnett's post hoc analysis on the main group effect (comparisons to control) See materials and methods for details on the lines. Running speeds over trials are represented as mean ± SEM with Tukey's trial-to-trial comparisons displayed as color-coded p-values. Statistical notations are as follows: 'ns' p > 0.05. (F) Running speed during trial 1 and 10 of hungry flies (24 h starved) lacking the Dop1R1 receptor gene and heterozygous controls. (G)

Average running speed during odor stimulation over 10 trials of hungry flies (24 h starved) without Dop1R1 compared to heterozygous controls (N=10/10, 2-way RM ANOVA p(trials)=0.0103; p(groups)=0.49, p(interaction)=0.59). The boxplot displays the main group effect of the ANOVA. (H) Circuit diagram. We modeled a population of KCs recurrently connected with DANs. Each population also receives self-feedback which indicates recurrent connections within the population. The odor input is delivered to both populations. An MBON integrates KCs and DAN activity and transforms it into running behavior. (I) Repeated odor presentation separated by odor-free intervals in the model. During each trial, odor presentation is represented as a step increase in the stimulus for 12 s. (J) Simulated KC/DAN activity for 10 consecutive trials separated by inter-stimulus intervals. During odor presentation (purple bar), DANs and KCs integrate the stimulus. Between stimuli, DAN and KC activity decreases due to the absence of input. The prolonged time constant that emerges in the recurrent circuit prevents neural activity from recovering to baseline during the inter-trial periods, resulting in its accumulation during subsequent stimulus presentation. (K) Optimized exponential transfer function transforms the neuronal activity of KCs and DANs in H into MBON activity. (L) Comparison between the MBON activity per trial obtained by the fitted model and the data (mean +/- SEM of starved flies in Fig. 3D). (M) Optimized exponential transfer function transforms the normalized MBON activity (relative to the data) into running speeds. (N) Running speeds as a function of trial number generated by the model. (O) Comparison between the average speed per trial obtained by the fitted model and the data (mean +/- standard error of the mean of Fig. 1E).